Composite Analyses of Wintertime Wind Stress Vector Fields with Respect to SST Anomalies in the Western North Pacific and the ENSO Events Part I. SST Composite

By Kimio Hanawa, Yasushi Yoshikawa and Tomowo Watanabe

Department of Geophysics, Faculty of Science, Tohoku University, Aoba-ku, Sendai 980, Japan
(Manuscript received 17 January 1989, in revised form 6 April 1989)

Abstract

Long-term wind stress vector (WSV) fields in winter over the North Pacific, which were calculated by Kutsuwada and Teramoto (1987), are analyzed by means of the composite method with respect to SST anomalies in the mid-latitudes of western North Pacific (SST composite). According to SST anomalies, two categorized winters, *i.e.*, warm and cold winters are selected during 24 years from 1961 to 1984. The numbers of warm and cold winters are six and five, respectively. In order to examine whether or not the composite WSV fields are well-ordered and/or rigid ones, maps of stability of WSV anomalies are constructed, and the new parameter, *Degree of similarity* of WSV anomaly field of each winter to the composited WSV anomaly field is introduced and discussed. Both parameters show that the extracted patterns for two categorized winters are well-ordered.

In warm (cold) winter, mid-latitudes westerly weakens (strengthens) and shifts northward (southward). As a result, the East Asian Winter Monsoon (*Kisetsuhu*) over Japan weakens (strengthens). It is also seen that in the equatorial region, in warm winter the region with SST higher than 28°C extends to the central to eastern part and its anomaly fields are very similar to those in ENSO year winter. Actually, winters selected as warm (cold) winter include the ENSO (ENSO+1) year winters, *i.e.*, winters during ENSO events, but not the ENSO+1 (ENSO) year winters.

Time series of *Degree of similarity* for westerly region to warm-winter composited WSV anomaly fields are well in agreement with those of "Far East zonal index", which is used by the Japan Meteorological Agency.

From the composite map for sea level pressures, it is shown that shifts of westerly axis correspond to north (warm winter)-south (cold winter) shifts of the Aleutian Low.

1. Introduction

Recently, many authors have pointed out that during an El Niño/Southern Oscillation (henceforth, ENSO) event, sea surface temperature (SST) in the mid- and high-latitudes of the North Pacific varies coherently with that in tropical region to some extent (*e.g.*, Iwasaka *et al.*, 1987, henceforth IHT1 ; Hanawa *et al.*, 1988, HWIST ; Kawamura, 1988 ; Yasunari, 1987a, b, 1988 ; Kitoh, 1988b). Among them, HWIST showed that during an ENSO event, positive SST anomalies in the ENSO year winter, *i.e.*, winter during an ENSO event (*e.g.*, January through March of 1983 for the 1982/83 ENSO event) appear in a wide zonal band along 30°N line, extending from the Asian coast to near 170°E, as shown in Fig. 1. On the other hand, in the following year winter, the distribution of SST anomalies is quite similar to that in the ENSO year winter with its sign reversed. This area with its characteristic appearance of anomalies agrees with one of sea areas partitioned by the cluster analysis for the long-term SST anomaly fields by Iwasaka *et al.* (1988, henceforth IHT2).

HWIST and Kawamura (1988) pointed out that one of causes of this characteristic variation of SST anomalies is attributed to the strength of the East Asian Winter Monsoon (*Kisetsuhu*) ; in general the East Asian Winter Monsoon in an ENSO year winter is weak compared with the other categorized winters.

The purposes of the present (Part I) and following (Part II by the same authors (1989b)) studies are to

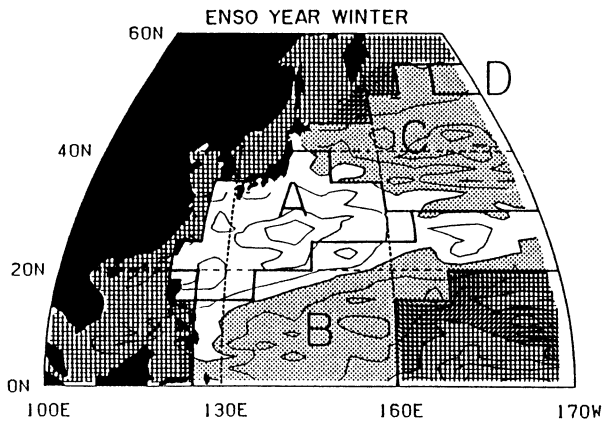

Fig. 1. Composited SST anomaly distribution in ENSO year winters. Regions A through D were specified by a cluster analysis made by Iwasaka *et al.* (1988). After Hanawa *et al.* (1988).

answer the following questions.

(1) Whether or not winters showing remarkably positive or negative SST anomalies in the mid-latitudes of western North Pacific are accompanied with their own characteristic wind fields over the North Pacific?

(2) Whether or not wind fields during ENSO events also show a characteristic feature even in mid- and high-latitudes?

(3) How are the results of cluster analysis by IHT2 and of composite analysis by HWIST for SST anomalies interpreted with respect to atmospheric wind forcing?

To answer the above questions, in the present study long-term wind stress vector (WSV) fields are examined by means of a composite method with respect to SST anomalies in the mid-latitudes of western North Pacific : *SST composite*. In the following paper, WSV fields will be also analyzed with respect to ENSO events following HWIST : *ENSO composite*. In both analyses, attention will be also paid to the Aleutian Low and the Siberian High by means of composite analysis for sea level pressure, since they may markedly affect the strength of the East Asian Winter Monsoon.

Recently, Kawamura (1988) performed the composite analyses for various meteorological elements with special reference to variation of surface air temperature over Japan in winter : cold and mild winters. He found that negative SST anomalies in the mid-latitudes are caused by the active wintertime monsoon, which associates with the anticyclonic circulation at the 200 hPa level over southern China. In addition, composite analysis for wind vectors at 700 hPa level showed that an elliptical anticyclonic (cyclonic) gyre centered on 40°N, 170°E appears over the North Pacific in mild (cold) winters. Although the present study treats WSVs, it is expected that the SST composite will show basically the same feature as wind vector fields at 700 hPa level found by Kawamura. However, it is noteworthy that since WSVs represent the atmospheric forcing (momentum flux) to the ocean, their distributions and variations can be connected directly to the oceanic spin-up or spin-down processes and indirectly to oceanic heat loss and mixing process in the upper ocean to some extent. Therefore, when our attention is paid to SST changes, WSV fields will be worthwhile analyzing.

The remainder of this paper is organized as follows : the data used are described in Section **2**. In Section **3**, climatological WSV fields and results of this SST composite for WSV fields are described in detail, and in Section **4**, a new parameter, *i.e.*, *Degree of similarity* is introduced and discussed. In Section **5**, the conditions of the Siberian High and the Aleutian Low are described based on the composited sea level pressure and their anomaly fields. In Section **6**, relationships of score of *Degree of similarity* to circulation indices around Japan and to variation of SST anomalies are discussed, and an interpretation of cluster analysis by IHT2 is given based on the present study. Section **7** gives a summary and remarks.

2. The data, selection of winters to be composited and stability of WSV

2.1. Data of wind stress vector (WSV) and sea level pressure (SLP)

Monthly mean WSV data are those calculated by Kutsuwada and Teramoto (1987). These data are arranged on a 2° × 5° (lat. × lon.) grid over the ocean area that covers almost the entire North Pacific from 120°E to 120°W and from the equator to 50°N with 564 grids (see Fig. 2a). The period is 24 years: from 1961 to 1984. The calculated original marine meteorological data are those compiled by the Japan Meteorological Agency (JMA). In their data for the equatorial region east from 170°W and south from 20°N the independent WSV data estimated by the Mesoscale Air-Sea Interaction Group, Florida State University were incorporated, since the compiled data by JMA are sparse there. The reader may refer to Kutsuwada and Teramoto (1987) for details.

For the present purpose, seasonal mean WSVs were calculated from the monthly data with those for December of the previous year, January and February regarded as the winter season of its year. Note that seasonal mean SSTs in HWIST were calculated with January, February and March regarded

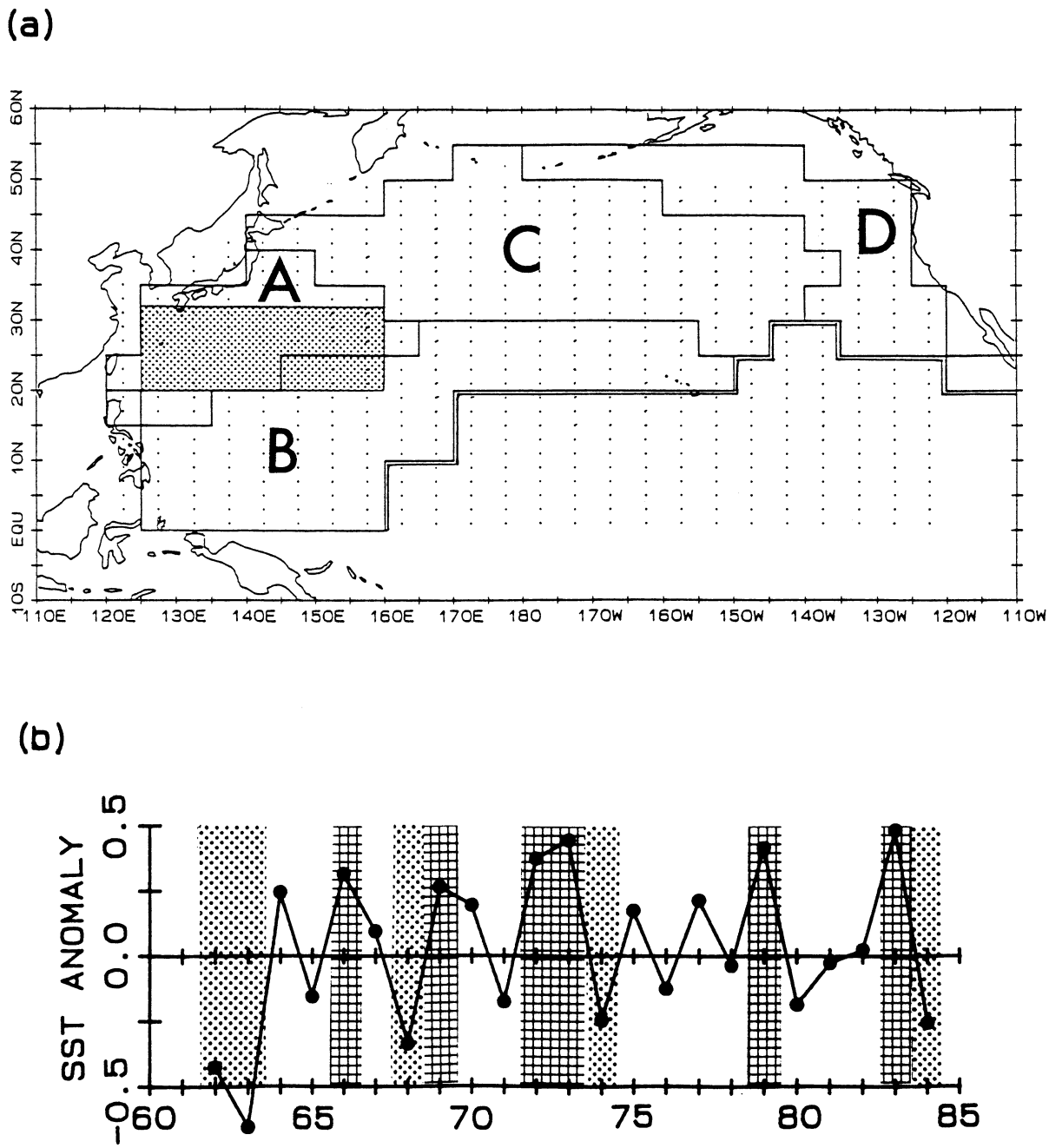

Fig. 2. (a) Area where time series of SST anomalies shown in (b) are calculated, which is superposed on borderlines of clusters given by Iwasaka *et al.* (1988). Note that the borderlines denoted by double lines represent the limit of the study area due to insufficient data. That is, the eastern end of Region B *etc.* is not clear. (b) Time series of SST anomalies averaged in the area specified in (a). Winters with hatches and dots denote warm and cold winters selected for composite analysis, respectively.

as the winter season. Although we also calculated seasonal mean WSVs in the same way as those of SSTs, it was judged that the results obtained from them were relatively unfavorable compared with those described in the present paper. This fact strongly suggests that WSV fields primarily cause variations of SST anomaly fields. Actually, IHT1 showed, from the lag correlation analysis, that the Pacific/North American (PNA) teleconnection pattern leads variations of SST anomalies in the mid-latitudes of the central North Pacific by one month.

Data of monthly SLP fields in the Northern Hemisphere used in Section 5 were provided by JMA. The data are given to a $10° \times 10°$ (lat. $\times$ lon.) grid for the Northern Hemisphere. The analyzed period is same as that of WSV fields, but since those in lowlatitudes do not cover the whole period mentioned above, the data for latitudes south of 20°N were not used. Seasonal mean values were also calculated as for WSVs.

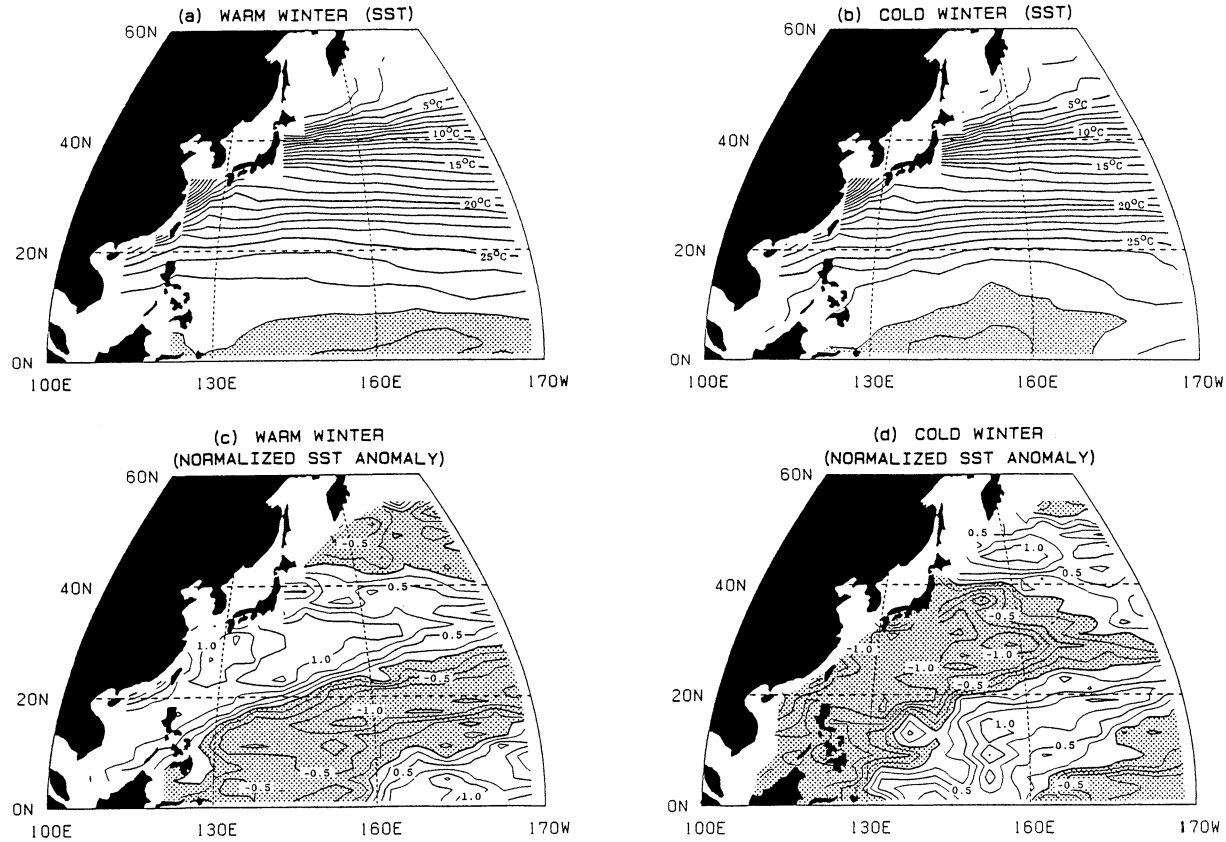

Fig. 3. Composite maps for SST fields for warm (a) and cold (b) winters, and their anomaly fields normalized by the standard deviation at each grid point for warm (c) and cold (d) winters. Contour intervals are 1°C in (a) and (b) and 0.25 in (c) and (d). The dotted areas denote the regions with SST higher than 28°C in (a) and (b), and with negative SST anomalies in (c) and (d).

2.2. Selection of winters to be composited

Figure 2b shows the time series of areal mean SST anomalies in the mid-latitudes of the western North Pacific: area specified in Fig. 2a. This area is regarded as the region where markedly positive SST anomalies appear in ENSO year winters as shown in Fig. 1 and is almost same as Region A described in IHT2. Winters with remarkably positive and negative SST anomalies, whose absolute values normalized by the standard deviation exceed about 0.8, were selected as shown in Fig. 2b. That is, six winters with highly positive SST anomalies are those in 1966, 1969, 1972, 1973, 1979 and 1983, while five winters with negative anomalies are those in 1962, 1963, 1968, 1974 and 1984. The numbers of selected winters as warm and cold winters are almost the upper a quartile and lower quartile of winters analyzed, respectively. In this paper, we call the former (latter) winters "warm (cold) winter".

Figures 3a through d show composite maps of SST fields for warm and cold winters and their anomaly fields normalized by the standard deviation at each grid point from climatology. These maps were made by the data same as HWIST. Comparing Fig. 3c with Fig. 1, pattern of anomalies are quite similar to each other in general features. However, the magnitude in the central regions showing positive or negative SST anomalies is much larger in a warm winter than in an ENSO year winter (see Fig. 2b of HWIST for normalized SST anomaly fields) and the northern boundary of the positive SST anomaly area shifts to about 45°N. The anomaly pattern in a cold winter is also very similar to that in a warm winter with the sign reversed and to that in ENSO+1 year winter (see Fig. 3 of HWIST). It should be noted here that the area specified in Fig. 2a to obtain the time series of Fig. 2b agrees well with the region showing highly positive or negative anomalies in warm or cold winters. Mean SST anomalies of the two categorized winters are 0.38°C and −0.38°C, respectively. Most of these selected winters in the 1970s and 1980s were same as those selected by Kawamura (1988) and Kitoh (1988a) based on surface air temperature over Japan in their studies.

2.3. Stability of WSV field

In order to examine whether or not composited WSV fields or WSV anomaly fields are well-ordered and rigid structures, the ratio of vector-averaging value of WSVs to their scalar-averaging value is cal-

culated at each grid point. This parameter, S, can be represented by the variability of WSV or WSV anomaly directions: if the WSVs to be composited point in only one direction, then S equals 1, and if directions of WSVs are random, S decreases towards zero, *i.e.*,

$$S = \frac{\left|\sum_{i=1}^{N} \mathcal{T}_i\right|}{\sum_{i=1}^{N} |\mathcal{T}_i|}, \quad 0 \leq S \leq 1,$$

where $\mathcal{T}_i$ is the WSV, and N is the number of WSVs to be composited. Contour maps of stability for composited WSV fields will give information on rigidity in structure to some extent. This non-dimensional parameter for wind velocity is called "Constancy" by Roll (1966) and "Stability of wind field" by Hanawa and Toba (1987). In this paper, we call this "*stability*" of WSVs or WSV anomalies.

3. Results of SST composite

3.1. Climatological mean winter WSV field

Figures 4a through c show the climatological mean winter WSV field, magnitude of WSVs, and stability of WSVs, respectively. The axis of the westerly lies along 40–35°N latitude line and it has a maximum wind stress of 0.20 Nm^{-2} around 165°E. The Low-latitudes easterly is strong along the 10°N line, especially from 175°W through 125°W, and east of the Philippine Islands they exceed 0.15 Nm^{-2}. The Intertropical Convergence Zone (ITCZ) can be seen clearly between 5°N and 7°N from the eastern part of the study area to the international date line. The borderline between westerly and easterly lies along the 25°N line and stability for this zonal band is extremely low. The anticyclonic gyre exists off California, U.S.A., but stability is low for this area. Stability is also low in the Doldrums. It is found that in general, the regions with relatively small WSVs correspond to those with low stability.

3.2. Composited WSV fields for two categorized winters

Figures 5a through c and 6a through c show WSV fields of warm and cold winters, their magnitude and their relative magnitude to climatological mean WSVs, respectively. Figures 7a through d are WSV anomaly fields from the climatological mean WSV field (Fig. 4a) and stability of WSV anomalies, respectively. From these basic figures, differences of WSV fields between the two categorized winters can be described as follows.

In the WSV anomaly fields of both categorized winters, well-organized features are seen not only in the easterly region but also in the westerly region.

In the WSV anomaly field of warm winter, an elliptical anticyclonic gyre centered on 40°N and the international date line appears in westerly region. As mentioned in the Introduction, this feature is basically same as the wind vector anomalies on 700 hPa level shown by Kawamura (1988, his Fig. 9). The existence of this gyre means the northward shift of the westerly axis as seen in Fig. 5a. In the mid-latitudes of the western North Pacific, *i.e.*, around Japan, northwestward WSV anomalies appear. This means the weakening of the East Asian Winter Monsoon (*Kisetsuhu*). This WSV pattern appearing in mid-to high-latitudes is also very similar to that obtained in GCM simulation by Kitoh (1988a). In his model, perpetual January warm SST anomalies are located in the western subtropical gyre, *i.e.*, the sea south of Japan.

On the other hand, in the equatorial region westerly anomalies appear east of 170°E along the equator. In the easterly region east of the international date line, a strong blow into the equator is prominent. This reflects that the region with SST higher than about 28°C, which usually locates around the Doldrums and the Maritime Continent, tends to extend east of the international date line in this categorized winter (see Fig. 3a). In general, this shift occurs during ENSO events. Actually, in this SST composite, three ENSO year winters are selected as warm winters, *i.e.*, 1966, 1973 and 1983.

It is very interesting that in the western part of the tropical Pacific, a strong blow towards the Maritime Continent appears, but east and north of Philippine Islands northward WSV anomalies exist. The former anomalies may mean the reduction of the Doldrums in area and consequently the direct blow of easteries over the Maritime Continent. Since stability is very high, it is considered that this structure is rigid. However, at this stage, what corresponds to this borderline is unknown.

Northwestward WSV anomalies appearing around Japan and northward WSV anomalies appearing east and north of the Philippine Islands mean that the East Asian Winter Monsoon in the whole mid-latitudes of western North Pacific weakens in a warm winter.

In a cold winter, the situation is almost reversed from that of warm winter. That is, and elliptical cyclonic gyre appears in the westerly region, which conversely means the southward shift of the westerly axis. Large southeastward to eastward WSV anomalies exist from the western part of the basin (near Japan) and to the international date line. In the most western part south of 20°N, southward WSV anomalies appear. That is, they represent a much stronger East Asian Winter Monsoon than that in a warm winter and strong northerlies blow to the Maritime Continent. In the easterly region, except for the most western part and the equatorial region from 160°E to the international date line, the easterly weakens. Exceptional WSV anomalies in the two regions direct towards the Doldrums. This suggests that the convergence region of wind, *i.e.*, con-

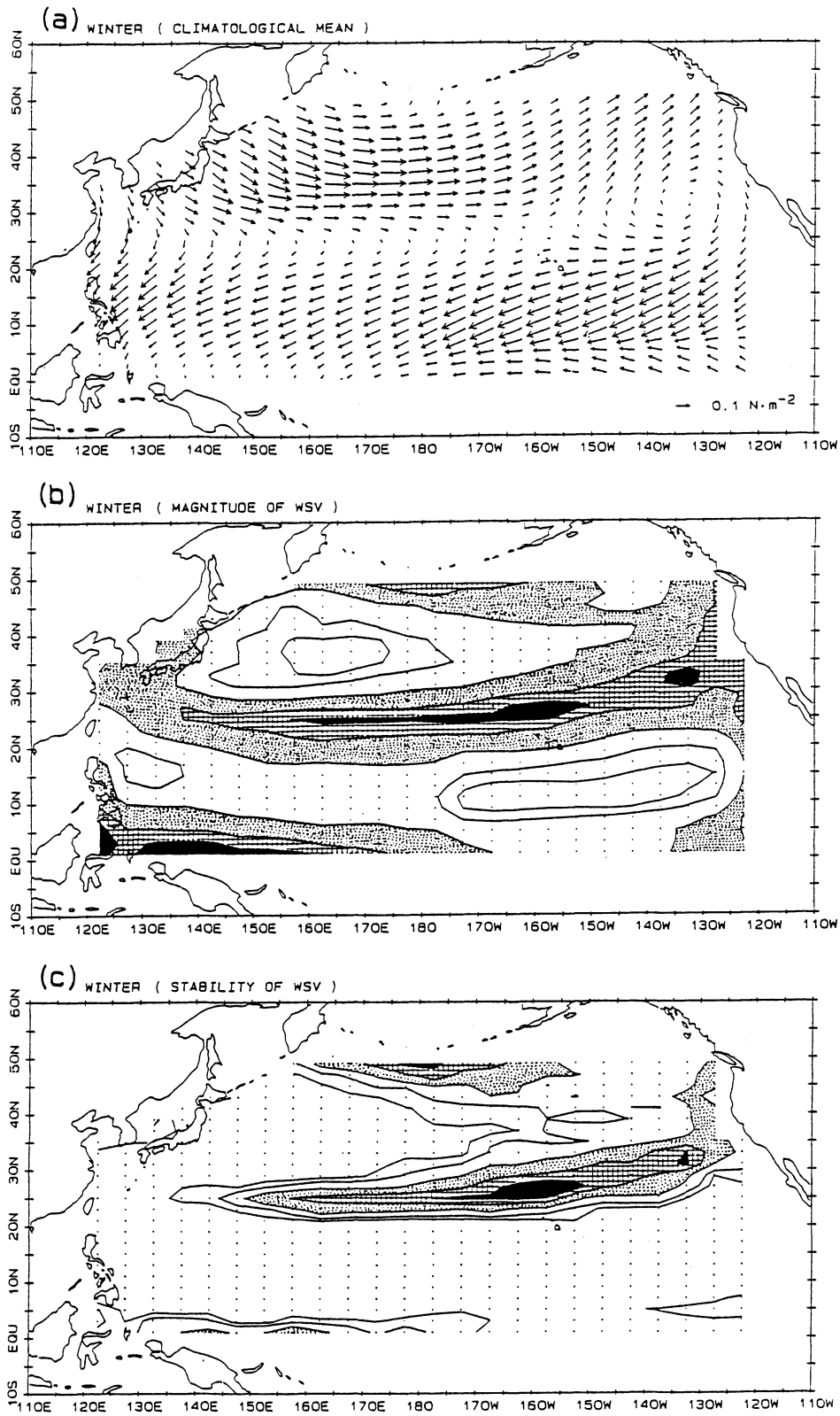

Fig. 4. Climatological mean winter WSV fields. (a) WSV field. Units of arrow lengh are is shown in the lower right corner. (b) Contour map of the magnitude of WSVs. The blackened, hatched and dotted areas represent the regions with values less than 0.025 Nm^{-2}, to 0.05 Nm^{-2} and to 0.1 Nm^{-2}, respectively. The thick and thin solid lines denote 0.15 and 0.175 Nm^{-2}, respectively. (c) Contour map of the stability of WSV. The blackened, hatched and dotted areas correspond to the regions with values less than 0.4, to 0.6 and to 0.8, respectively. The thick and thin solid lines denote 0.9 and 0.95 contours, respectively.

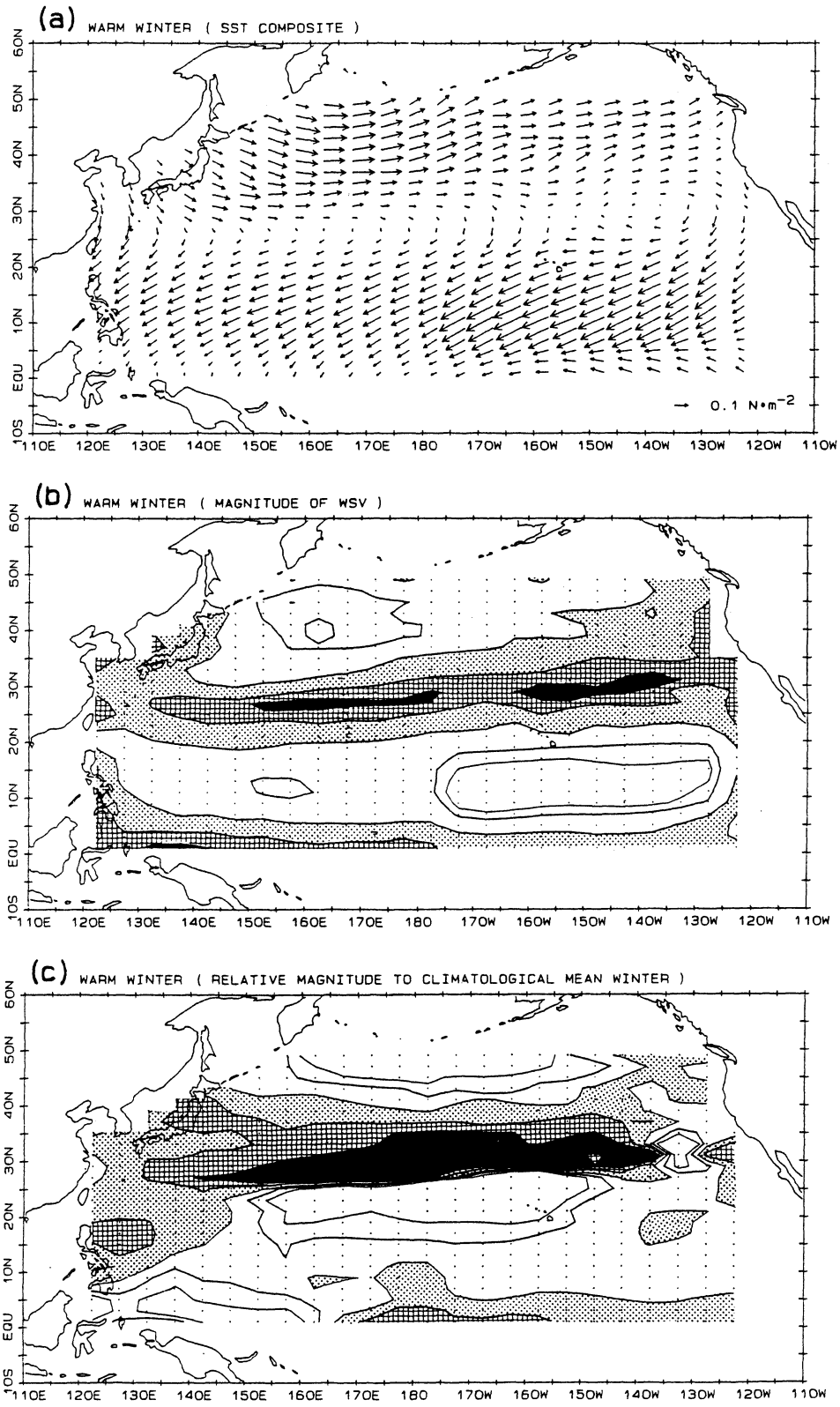

Fig. 5. Composited WSV fields for warm winter. (a) WSV field, (b) magnitude of WSVs and (c) relative magnitude of WSVs for climatological mean WSVs. Representations are same as Fig. 4(a) and (b) for WSV fields and magnitude of WSVs, respectively. In (c), the blackened, hatched and dotted areas correspond to the regions with values less than 0.6, to 0.8 and to 1.0, respectively. The thick and thin solid lines denote 1.2 and 1.4 contours, respectively.

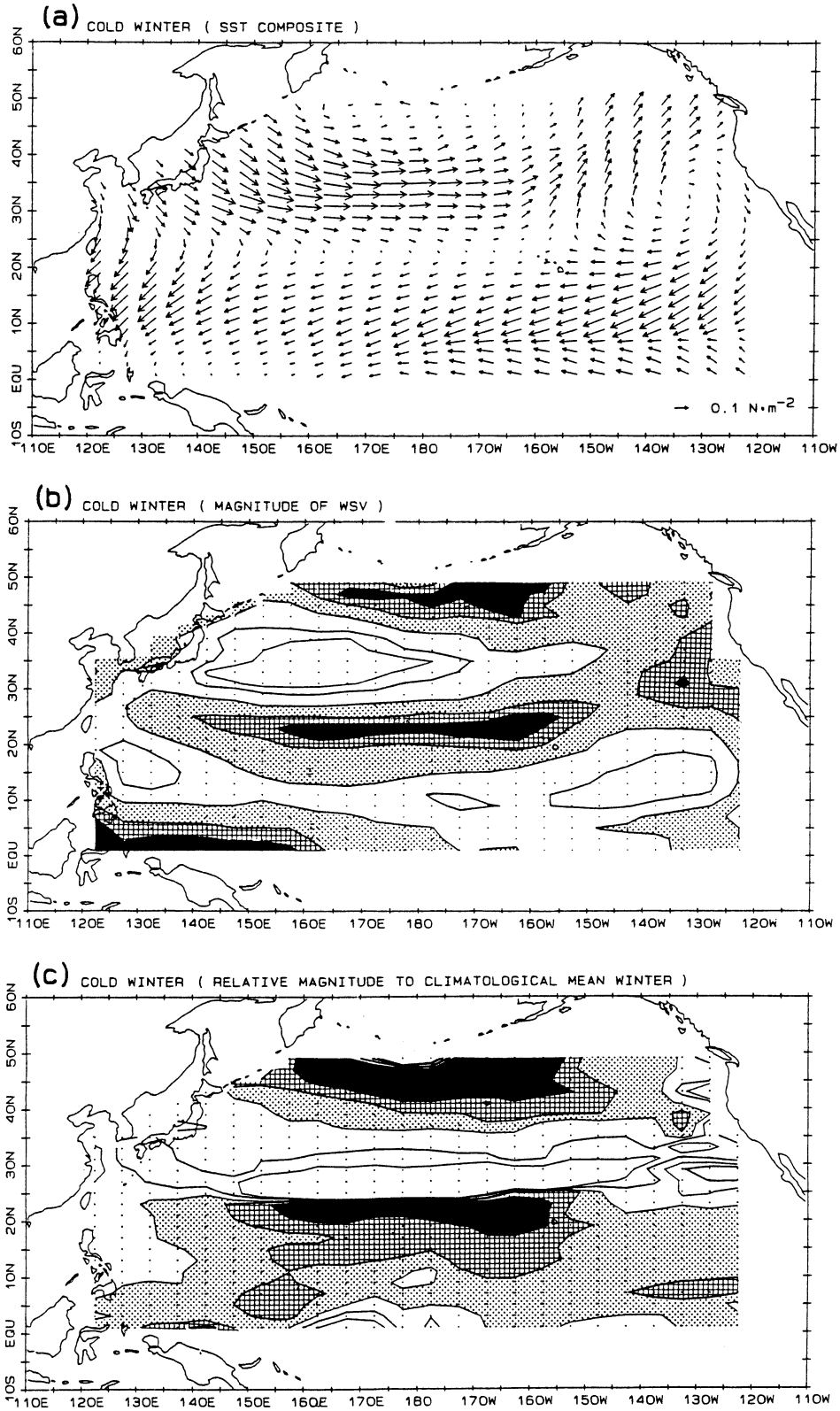

Fig. 6. Same as Fig. 5 but for cold winter.

vection region situates around the Doldrums and the Maritime Continent.

Distributions of the relative magnitude of two categorized winters to the climatological mean winter (Figs. 5c and 6c) show almost reversed features. In warm (cold) winter, WSVs strengthen (weaken) in regions north of about 40°N line and south of 25°N line, except for the westernmost part and the equatorial region. That is, easterlies and westerlies change their strength alternately.

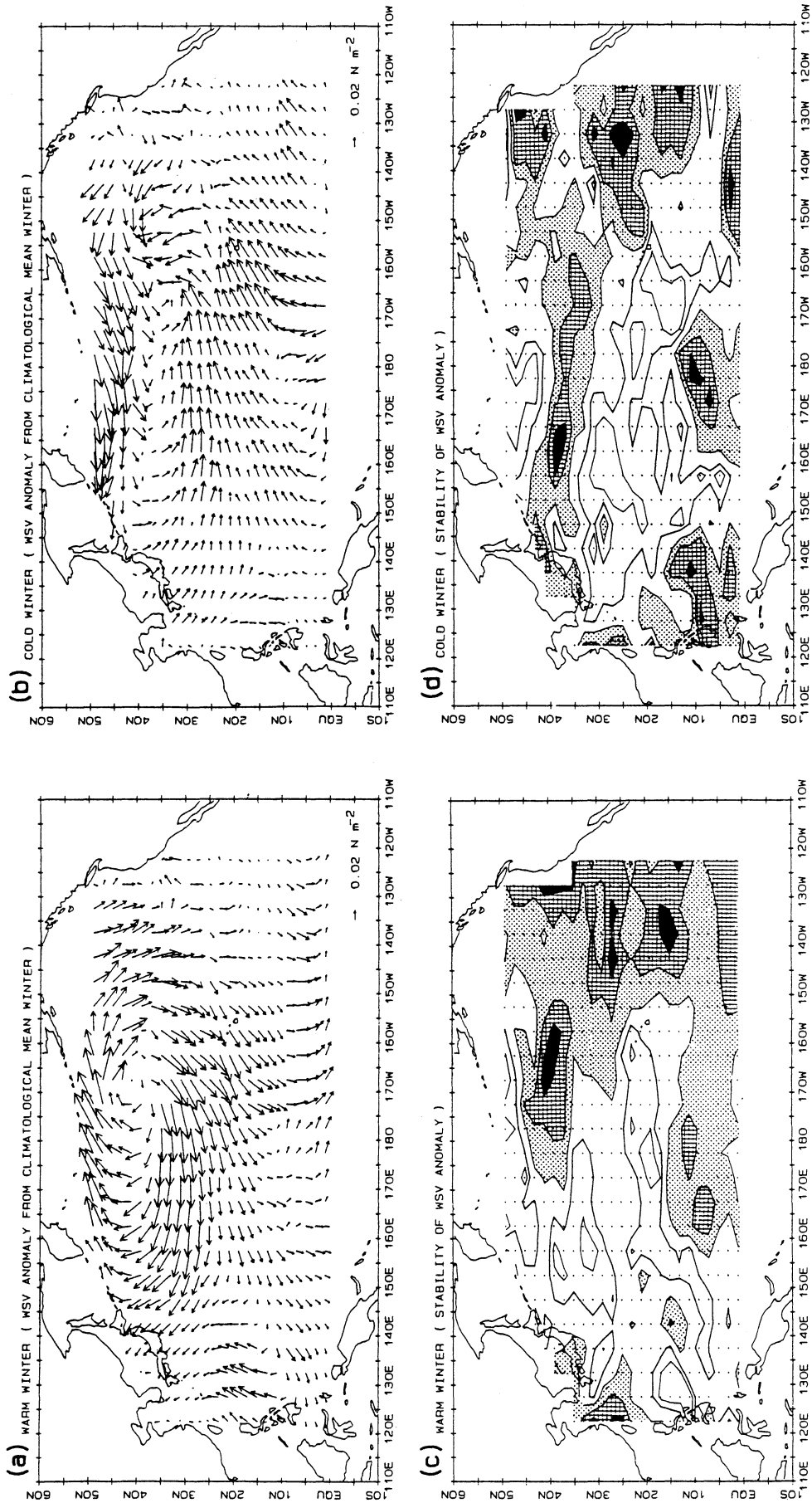

Fig. 7. WSV anomaly fields of warm (a) and cold (b) winters from climatological mean fields shown in Fig. 4 (a), and contour maps of stability of WSV anomalies for warm (c) and cold (d) winters. The blackened, hatched and dotted areas correspond to the regions with values less than 0.2, to 0.4 and to 0.6, respectively. The thick and thin solid lines denote 0.8 and 0.9 contours, respectively.

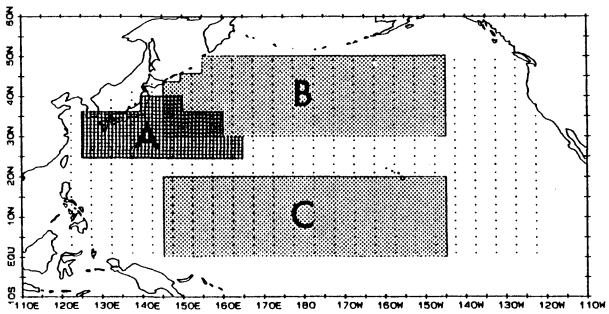

Fig. 8. Areas A, B and C where scores of *Degree of similarity* are calculated.

The stability of WSV anomalies is relatively high in almost the whole basin except for the eastern part and the region with small WSV anomalies. That is, it can be judged that composited WSV fields for both categorized winters have relatively strongly-built structures, especially in the region east and south of Japan.

4. Similarity of WSV anomaly fields of each winter to composited WSV anomaly fields

In the previous section, we presented the results of composited WSV fields for warm and cold winters. Although their well-ordered features were shown to some extent by using maps of the stability of WSV anomalies, there still remains the question as to what degree *WSV anomaly fields of each year.* are similar to WSV anomaly fields composited for warm and cold winters.

To assess this quantitatively, the new parameter of "*Degree of similarity*", F is introduced and calculated as one of the trials. That is, at each grid point, the cosine of the angle, θ between the composited WSV anomaly vector and the WSV anomaly vector of each winter is calculated, and then the areal average for notable regions is estimated. This average is the definition of *Degree of similarity.* Therefore, *Degree of similarity* can take both positive and negative scores:

$$F = \left(\frac{1}{N}\right)\sum_{i=1}^{N}(\cos(\theta_i)), \quad -1 \leq F \leq 1,$$

where N is the number of grid points for some notable region. If this *Degree of similarity* has a highly positive score, then pattern of WSV anomaly fields of its winter can be judged to be very similar to that of composited WSV anomaly fields: when it has a highly negative score, then WSV anomaly vectors direct to almost the opposite side to the composited WSV anomaly vectors.

This idea is based on the assumption that WSV anomalies tend to appear in the same pattern irrespective of amplitude. That is, it is to be postulated that the dynamics causing WSV anomalies is basically the same. Although the magnitude of WSV anomalies could be taken account of by the inner (scalar)-product of WSV anomalies of each winter and composited WSV anomalies, this approach was unsuccessful. This is because the contribution to scores from the magnitude of WSV anomalies is superior to that based on the direction of WSV anomalies.

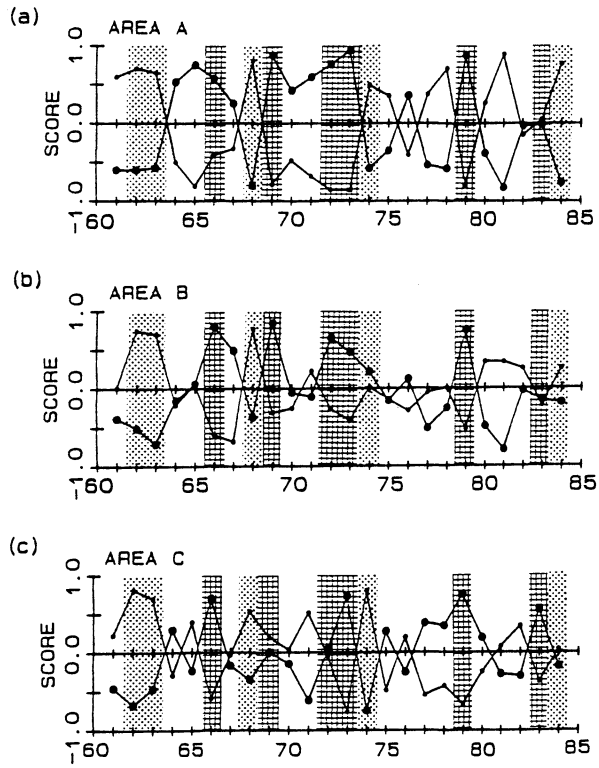

Fig. 9. Time series of scores of *Degree of similarity* for three areas. (a) Area A, (b) Area B and (c) Area C. Large (small) closed circles denote those of warm (cold) winter.

The *Degree of similarity* is calculated for three areas shown in Fig. 8. Area A is almost the same region as Region A of IHT2 and the area experienced SST anomalies as shown in Fig. 2b. Areas B and C correspond to the main parts of the westerly and easterly regions, respectively.

First, scores of *Degree of similarity* of WSV anomaly fields in warm winter to those in cold winter were calculated for the above three areas. Those are −0.95 for Area A, −0.66 for Area B and −0.80 for Area C. This means that in whole the basin, especially in Area A, WSV anomalies direct to almost opposite sides between the two categorized winters.

Figures 9a, b and c show the time series of scores of *Degree of similarity* for Areas A, B and C, respectively. In Area A, since the score of *Degree of*

similarity of the WSV anomaly of the warm winter to that of the cold winter is −0.95 as mentioned above, these two time series of scores are almost symmetrical to the horizontal axis. In addition, it is found that since the selected warm or cold winters to be composited have generally high scores, this composite is reasonable. However, there are a few exceptions. For example, although the 1983 winter was selected as a warm winter, the score is very low and the 1974 winter, which was regarded as cold winter, is also low. On the other hand, those for the 1965, 1971 winters are very high for warm winters and those of the 1978 and 1981 winters are high for cold winters.

In Areas B and C, scores of *Degree of similarity* are low compared with those of Area A. Nevertheless, scores for winters used in the composite are relatively high. That is, it shows that structures extracted by this analysis are well-ordered ones with a basin scale. Here it should be noted that in Area C, ENSO year winters (those in 1964, 1966, 1970, 1973, 1977 and 1983) show high scores for WSV anomalies of warm winter. As pointed by HWIST, this agrees with the fact that in ENSO year winters, SST anomalies have positive values in Region A of IHT2.

5. The Siberian High and the Aleutian Low

In order to show the conditions of SLP fields for the two categorized winters, in this section we present SLP fields of the Northern Hemisphere by means of a composite analysis with special reference to the AL and the Siberian High (SH).

The behavior of the Aleutian Low (AL) is investigated by many authors. Among them, Frits (1985) analyzed the positions of the AL for two categorized winters, *i.e.*, warm and cold SSTs in the eastern tropical Pacific. He pointed out that when in a high (low) SST winter, the central pressure of the AL is low (high) and its center situates east (west) of the international date line. In general, winters with high SSTs in the eastern tropical Pacific correspond to the ENSO year winter (Rasmusson and Carpenter, 1982). Recently, Rienecker and Ehret (1988) analyzed the wind stress curl over the North Pacific, and pointed out that most remarkable variations of it are associated with the east-west oscillation of the AL.

Figures 10a through c show the climatological mean SLP fields and composited ones for warm and cold winters, respectively. Figures 11a and b show the distribution of anomalies normalized by the standard deviation at each grid point for warm and cold winters, respectively. In climatological SLP fields, one high and two lows appear: the SH, the AL and the Icelandic Low, respectively. Between the two lows, a weak ridge lies over the North American Continent.

It is seen that in a cold winter, the SH develops more than in a warm winter. In a warm winter, the SH center is 50°N and 90°E and its SLP is 1036.6 hPa, while in cold winter it is 50°N and 100°E with 1039.2 hPa. Since the data are given on a 10° × 10° grid, it must be noted that the exact centers of high or low are not accurately located. Nevertheless, the two maps of Fig. 10c suggest the eastward shift and development of the SH in cold winter.

On the other hand, in a warm winter, the center of the AL is located at 50°N and 170°E with 1001.3 hPa, but in a cold winter the location of minimum SLP of 1000.1 hPa is same as that in a warm winter. Although the difference in magnitude between ALs for the two categorized winters in not clearly seen from the map, the southward shift of the AL center in a cold winter is remarkable. As a result, over the Western North Pacific, especially over Japan, the horizontal pressure gradient steepens in a cold winter and it corresponds to the strengthening of the East Asian Winter Monsoon.

The above-mentioned conditions can be also seen in the distribution of normalized SLP anomalies shown in Fig. 11. In a warm winter a negative region over the East Asian Continent and a highly (exceeding one standard deviation) positive region over the North Pacific appear, corresponding to a weakening of the East Asian Winter Monsoon. In a cold winter, the situations are almost reversed. In respect of the North Pacific, a difference of anomaly patterns in warm or cold winters means the northward or southward shift of AL.

It is interesting to point out that SLPs of the AL for the two categorized winters are higher than that of climatological mean value of 999.7 hPa. It suggests that in the winters not selected as the two categorized winters, a remarkable development of AL occurred. In addition, there are two centers in the Icelandic Low in a cold winter. This may reflect that one high and two lows coherently change simultaneously to some extent. As mentioned above, since the variability of the SH or AL is large and the behavior of both the SH and AL are very important in determining the wind forcing fields over the North Pacific, more detailed and comprehensive studies will be needed.

6. Discussions

6.1. Score of Degree of similarity and circulation indices

It is noteworthy that the time series of *Degree of similarity* for Areas A and B for warm winter anomaly fields are in good agreement with those of "Far East zonal index" (ZOI). This index, which is defined by the mean difference of geopotential height at 500 hPa level between 40°N and 60°N from 90°E to 170°E is regarded as a condition of the mid-latitudes westerly, and is commonly referred to by the Japan Meteorological Agency (see, *e.g.*, Nomoto

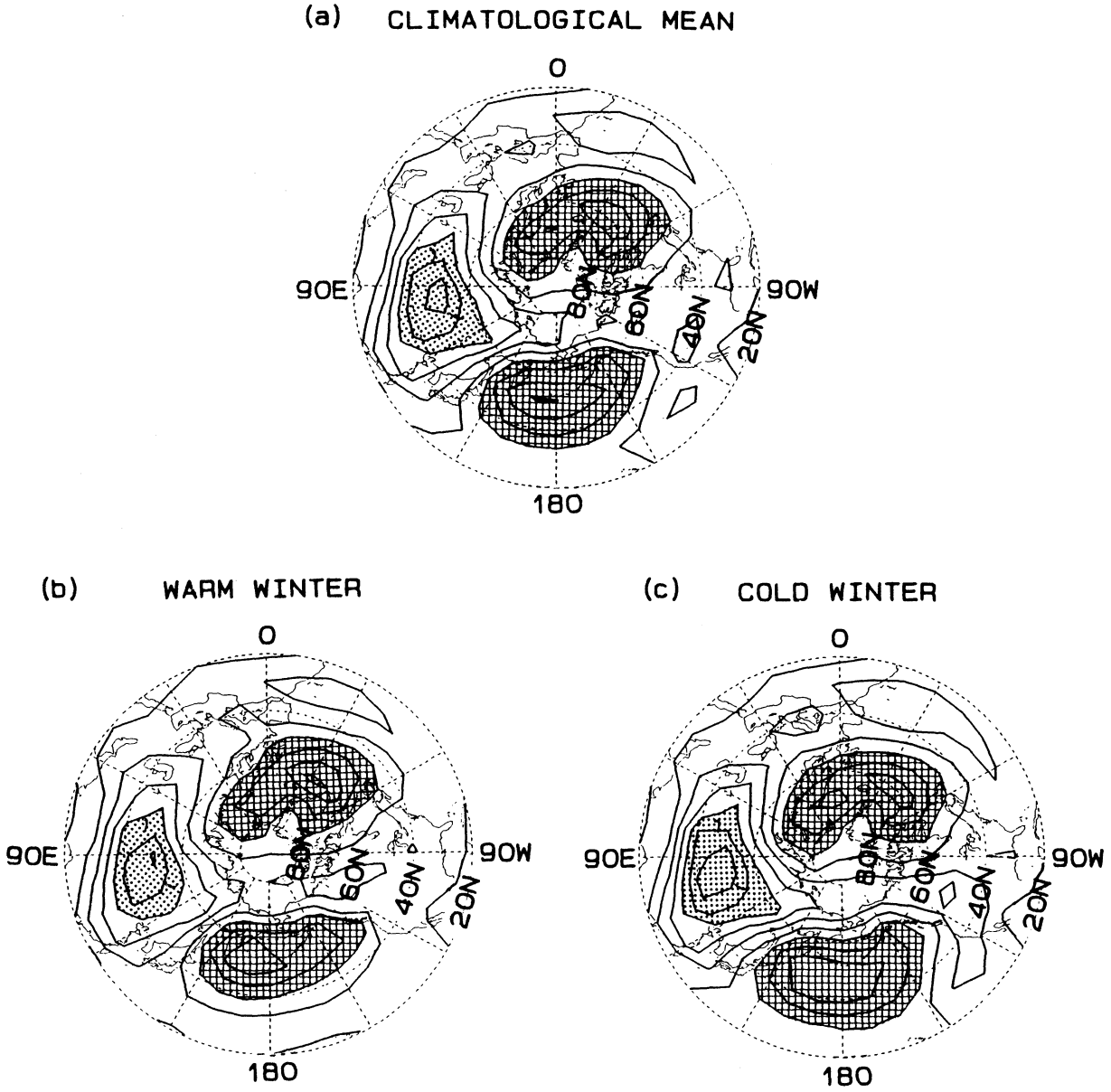

Fig. 10. Climatological mean (a) and composited SLP fields of warm (b) and cold (c) winters. Contour interval is 4 hPa. The dotted (hatched) areas correspond to the regions where SLPs are higher (lower) than the value of 1028 (1012) hPa.

and Chiba 1986). Figure 12 shows the time series of *Degree of similarity* for Area B, *i.e.*, westerly region, and ZOI. The correlation coefficient between them is 0.84. Therefore, scores in Areas A or B has the same meaning as ZOI, and the low (high) scores of ZOIs represent the southward (northward) shift of the westerly axis.

In addition, the correlation coefficient between the monsoon index (MOI, see HWIST) and scores for Area A for warm (cold) winter anomaly fields is −0.63 (0.61), whose absolute value exceeds 0.52 at the 99 % significance level of correlation coefficient with 22 degrees of freedom by the *t*-test. Therefore, it can be concluded that this score as well as this index can also represent the strength of the East Asian Winter Monsoon.

6.2. Interpretation of results of cluster analysis by IHT2

Figure 13 shows the WSV difference between warm and cold winters : WSVs in a cold winter minus those in a warm winter. Borderlines of clusters given by IHT2 are superposed on it.

Region A corresponds to the area where the East Asian Winter Monsoon changes considerably. As mentioned in the following subsection, although magnitude of SST anomalies in this region does not correspond exactly only to that of WSV anomalies, it is shown that they are governed by the strength of East Asian Winter Monsoon to a great

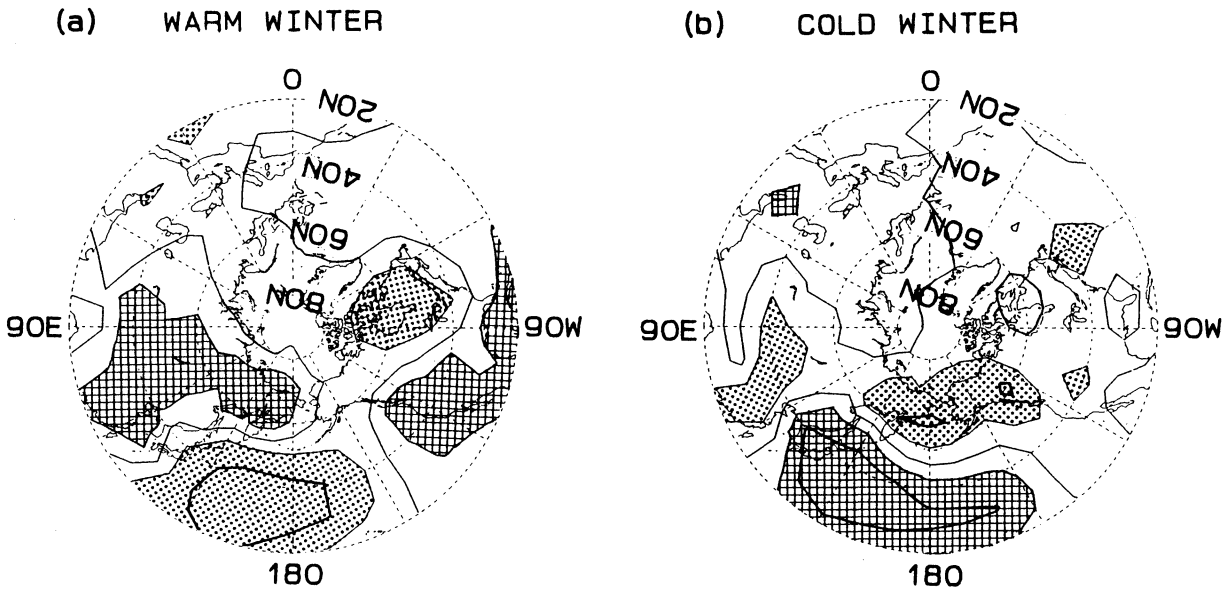

Fig. 11. Anomaly fields normalized by the standard deviation at each grid point for warm (a) and cold (b) winters. Contour interval is 0.5. The dotted (hatched) areas correspond to the regions where anomalies are higher (lower) than 0.5 (−0.5).

extent. Therefore, it can be concluded that suggestions of a relationship between SST anomalies and the East Asian Winter Monsoon by IHT2, HWIST and Kawamura (1988) are confirmed by the present study.

Region B whose SST anomaly varies in a seesaw-like manner with respected to Region A in winter, corresponds to the blow of an easterly into the atmospheric convection region around the Doldrums and the Maritime Continent. That is, the magnitude of WSVs weakens in a cold winter and strengthens in a warm winter. Since the magnitude of WSVs associates with heat loss and causes the deepening of mixed layer by the entrainment process from the lower layer, the relationship between SST anomalies and WSV anomalies is reasonable. Although the surface Ekman transport is one of the candidates causing SST warming (lowering) in a cold (warm) winter, this must be excluded at least for the low-latitudes and the equatorial region because its direction of advection is in the opposite sense. That is, in a cold winter showing a positive SST anomaly, the Ekman transport is southward (advection of low temperature water in the mid-latitudes) and vice versa.

Region C of IHT2 agrees with the northern three-quarters of an anticyclonic gyre in the present map. IHT2 showed that some portion of SST variation in Regions C and D is affected by the Pacific/North American (PNA) teleconnection pattern. In general, the PNA pattern tends to appear during the winter of ENSO events, although exceptional cases exist such as winter of the 1972/73 ENSO event as

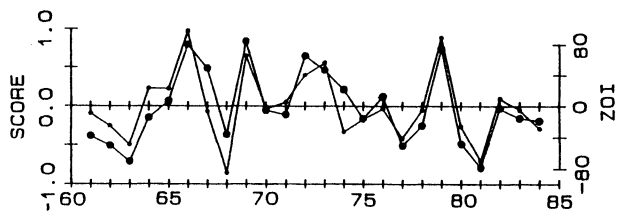

Fig. 12. Time series of scores of *Degree of similarity* for Area B to warm winter WSV anomaly field and those of "Far East zonal index" (ZOI). Large and small closed circles show those of score of *Degree of similarity* and ZOI, respectively. Units are m for ZOI. This index is used by JMA as indicator of the westerly condition. The vertical axis is arbitrary.

pointed out by IHT1. When a PNA pattern is excited, a low pressure anomaly appears with its center on 50°N and 170°W and high pressure appears over Alaska at 500 hPa level. However, since the southern boundary of the negative SST anomaly area in a warm winter (Fig. 3c) shifts northward compared with that of an ENSO year winter (Fig. 1), and PNA signals are not clearly seen in SLP anomaly fields (Fig. 11a), an alternative interpretation must be sought for the present result.

More recently, Iwasaka (1988) showed that the time series of SST anomalies in mid-to high-latitudes of the central Pacific highly correlates with that of the zonal component of wind stress and the friction velocity three cubed. That is, this means that

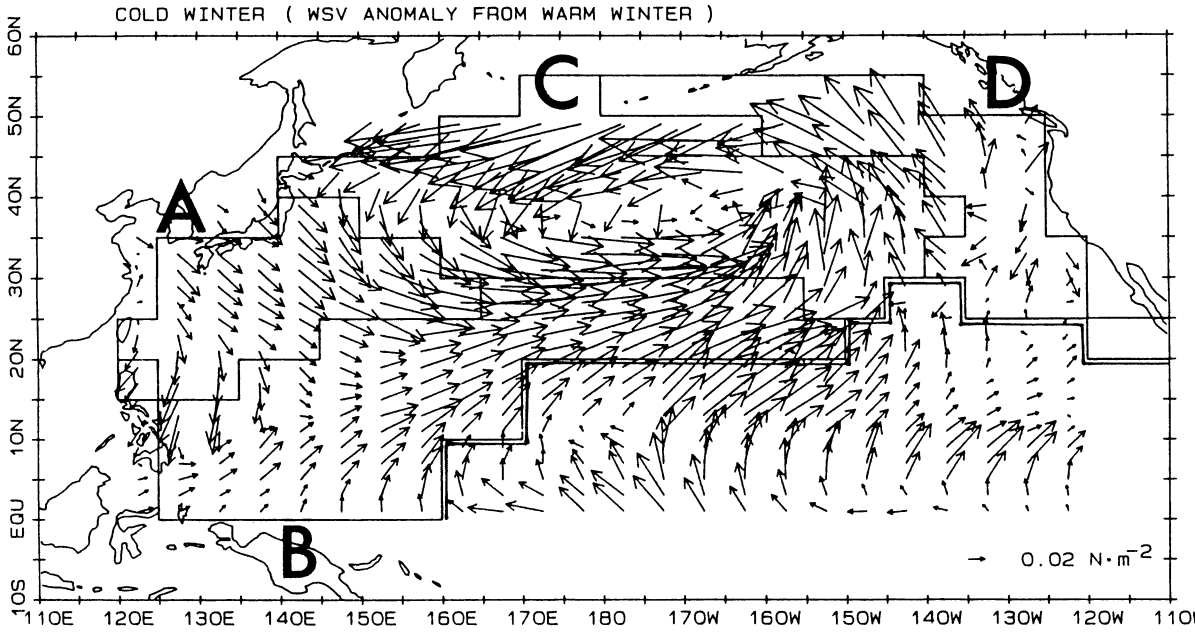

Fig. 13. Difference vectors between composited WSVs for warm winter and those for cold winter. The borderlines of clusters specified by cluster analysis of IHT2 are superposed.

SST anomalies in this region are determined by the north-south Ekman transport as well as the mixing process. Since in warm (cold) winters negative (positive) anomalies appear just under the westerly region as shown in Fig. 3c and d, Iwasaka's interpretation can reasonably be applied to our results.

6.3. Comparison of the time series of SST anoma- and the Degree of similarity

Since we could make a time series of *Degree of similarity* for the two categorized winters, it is interesting to compare it with an SST anomaly time series . Figure 14 shows the time series of the SST anomaly (Fig. 2b) and the *Degree of similarity* of Area A for a warm winter (Fig. 9a). It can be said that both time series agree with each other as a whole. However, in 1965, 1971, the latter years of the 1970s, 1981 and 1983, they show large differences or they have an opposite sign. In addition, it is noteworthy that in winters before the mid 1970s, SST anomalies decreased more than wind anomalies, while in the winters after the SST anomalies did not lower. This disagreement and variability may be due to the effect of large-scale oceanic heat transport. That is, both effects of air-sea interaction and oceanic heat transport are important in determining SST in the mid-latitudes of the Western North Pacific.

Recently, Kashiwabara (1987) pointed out that the ZOI lowered from the late 1970s to mid 1980s, which can be seen in Fig. 12 in the present paper. Nitta and Yamada (1989) also showed the decadal variations in SST fields as well as pressure and OLR

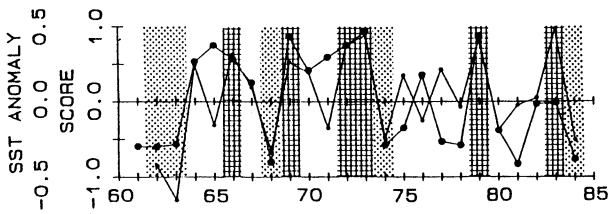

Fig. 14. (a) Time series of scores of *Degree of similarity* of each winter in Area A for warm winter (Fig. 9 (a)) and those of SST anomaly (Fig. 2 (b)). Large and small closed circles show those of score of *Degree of similarity* and SST anomaly, respectively. The vertical axis is arbitrary.

fields over the globe and pointed out that from the late 1970s through 1980s equatorial SSTs become warmer and these is significant lowering of the geopotential height at 500 hPa in the North Pacific during winter. All these facts, including the present study, suggest the existence of strong several-year to decadal signals in the North Pacific SST fields and atmospheric circulation in the Northern Hemisphere.

7. Summary and remarks

Long-term WSV fields in winter over the North Pacific, which were prepared by Kutsuwada and Teramoto (1987) were analyzed from the viewpoint of SST anomalies in the mid-latitudes of the western Pacific.

The main results can be summarized as follows.

(1) WSV anomaly fields causing SST anomaly variations in the mid-latitudes of the western North Pacific have the basin scale structures.

(2) In warm (cold) winter when remarkable positive (negative) SST anomalies appear in the mid-latitudes of western North Pacific, the axis of the mid-latitudes westerly moves northward (southward). Correspondingly, the easterly in low-latitudes strengthens (weakens) and is associated with change of positions of the convection region.

(3) With reduction (development) of the Siberian high in a warm (cold) winter, the center of the Aleutian low moves northward (southward). These changes are responsible for those of the WSV fields mentioned above.

(4) The results of cluster analysis for SST anomalies in the North Pacific made by IHT2, especially Regions A and B, can be reasonably interpreted from the changes of WSV fields.

As mentioned in the Introduction, WSV fields directly correspond to oceanic circulation. For example, the difference of the position of the westerly axis between warm and cold winters means a difference in the position of the zero line of wind stress curl. That is, in a cold winter, boundary of the subpolar and subtropical oceanic circulations shifts southward in the western and central Pacific. As pointed by Sekine (1988a, b), the southward excursion of the Oyashio First Intrusion east of Japan may be governed by changes of in this atmospheric forcing. In addition, the strengthening or wakening of easterly and westerly reflects on the Sverdrup volume transport and as its consequence the western boundary current, *i.e.*, the Kuroshio. Since the oceanic current is able to transport and redistribute a large amount of heat, the oceanic response to WSV fields must be taken into account for clarification of relatively low frequency SST variations.

In the accompanying paper (Part II), we will present the results of ENSO composite.

Acknowledgment

The authors wish to express their sincere thanks to Prof. Y. Toba and other members of Physical Oceanography Laboratory, Tohoku University for their useful comments and discussion. They also thank Dr. K. Kutsuwada, who kindly provided the wind stress data set and made useful comments. Thanks are extended to the Long-range Forecast Division, Forecast Department of the JMA for providing the sea level pressure data set. Comments by two anonymous reviewers have been useful in improving the manuscript.

This study was made as part of OMLET (Chairman: Prof. Y. Toba), one of the Japanese WCRP activities, which was financially supported by the Japanese Ministry of Education, Science and Culture. The first author (KH) was also financially supported by the Japanese Fisheries Agency, in the special research project, "Oyashio Region".

References

Frits, S., 1984 : The Aleutian Low in January and February-Relation to Tropical Pacific sea surface temperature. *Mon. Wea. Rev.*, **113**, 271–275.

Hanawa, K. and Y. Toba, 1987 : Critical examination of estimation methods of long-term mean air-sea heat and momentum transfers. *Ocean-Air Int.*, **1**, 79–93.

Hanawa, K., T. Watanabe, N. Iwasaka, T. Suga and Y. Toba, 1988 : Surface thermal conditions in the western North Pacific during the ENSO events. *J. Meteor. Soc. Japan*, **66**, 445–456.

Hanawa, K., Y. Yoshikawa and T. Watanabe, 1989 : Composite analyses of wintertime wind stress vector fields with respect to SST anomalies in the western North Pacific and the ENSO events. Part II. ENSO composite. Submitted to *J. Meteor. Soc. Japan.*

Hays, W.L., 1981 : *Statistics* (3rd Edit.). Holt-Saunders International Editors, 723pp.

Iwasaka, N., K. Hanawa and Y. Toba, 1987 : Analysis of SST anomalies in the North Pacific and their relation to 500mb height anomalies over the Northern Hemisphere during 1969-1979. *J. Meteor. Soc. Japan*, **65**, 103–114.

Iwasaka, N., K. Hanawa and Y. Toba, 1988 : Partition of the North Pacific based on similarity in temporal variations of the SST anomaly. *J. Meteor. Soc. Japan*, **66**, 433–443.

Iwasaka, N., 1988 : Variation of sea surface temperature and surface heat fluxes in the North Pacific. Doctoral thesis, Tohoku University, 242pp.

Kashiwabara, T., 1987 : On the recent winter cooling in the North Pacific. *Tenki*, **34**, 777–781 (in Japanese).

Kawamura, R., 1988 : The interaction between winter monsoon activities in East Asia and sea surface temperature variations over the western Pacific ocean. *Geophys. Rev. Japan*, **61** (Ser. A), 469–484 (in Japanese with English abstract and captions).

Kitoh, A., 1988a : A numerical experiment on sea surface temperature anomalies and warm winter in Japan. *J. Meteor. Soc. Japan*, **66**, 515–533.

Kitoh, A., 1988b : Correlation between the surface air temperature over Japan and the global sea surface temperature. *J. Meteor. Soc. Japan*, **66**, 967–986.

Kutsuwada, K. and T. Teramoto, 1987 : Monthly maps of surface wind stress fields over the North Pacific

during 1961-1984. Bull. Ocean Res. Insti., Univ. Tokyo, No. 24, pp100.
Nitta, T. and N. Yamada, 1989 : Recent warming of tropical sea surface temperature and its relationship with Northern Hemisphere circulation. *J. Meteor. Soc. Japan*, **67**, in press.
Nomoto, S. and M. Chiba, 1986 : Relation between the monthly mean temperature, monthly total precipitation and the 500mb circular indices in Japan. *Tenki*, **33**, 593–601 (in Japanese).
Rasmusson, E.M. and T.H. Carpenter, 1982 : Variations in tropical sea surface temperature and surface wind fields associated with the Southern Oscillation/El Nino. *Mon. Wea. Rev.*, **110**, 354–384.
Rienecker, M.M. and L.L. Ehret, 1988 : Wind stress curl variability over the North Pacific from the Comprehensive Ocean-Atmosphere Data Set. *J. Geophys. Res.*, **93**, 5069–5077.
Roll, H.V., 1965 : Physics of Marine Atmosphere, New York, Academic Press, pp426.
Sekine, Y., 1988a : Anomalous southward intrusion of the Oyashio east of Japan. 1. Influence of the seasonal and interannual variation in the wind stress over the North Pacific. *J. Geophys. Res.*, **93**, 2247–2255.
Sekine, Y., 1988b : A numerical experiment on the anomalous southward intrusion of the Oyashio east of Japan. Part I. Barotropic model. *J. Oceanogr. Soc. Japan*, **44**, 60–67.
Yasunari, T., 1987a : Global structure of the El Nino/Southern Oscillation. Part I. El Nino composites. *J. Meteor. Soc. Japan*, **65**, 67–80.
Yasunari, T., 1987b : Global structure of the El Nino/Southern Oscillation. Part II. Time evolution. *J. Meteor. Soc. Japan*, **65**, 81–102.
Yasunari, T., 1988 : Impact of Indian monsoon on the ocean mixed layer temperature in the Tropical Pacific. Submitted to *J. Climate*.

西部北太平洋の海面水温アノマリとENSOイベントに関する冬季の海面風応力ベクトルの合成図解析
Part I. 海面水温変動に対する解析

花輪公雄・吉川泰司・渡邊朝生
（東北大学理学部地球物理学教室）

Kutsuwada and Teramoto (1987) が評価した北太平洋上の海面風応力場を、西部北太平洋中緯度日本近海の海面水温アノマリに着目して、合成図解析手法により解析した。1961年から1984年の24年間の冬季から、海面水温アノマリにより、暖かい冬 (WW) と寒い冬 (CW) のふたつのカテゴリの冬季を、それぞれ6冬季、5冬季選んだ。解析では、合成された風の応力場が、良く組織化されたものであるかを検討するため、気候値からのアノマリベクトルの安定度の図を示した。また、今回新たに、各年の冬季の風の応力場の気候値からのアノマリが、上記ふたつのカテゴリで合成された風の応力場の気候値からのアノマリとどの程度パターンが似ているかを示す、「相似度」なるパラメータを定義して評価した。その結果、ふたつのカテゴリで合成された海面風応力場は、安定度が広い海域で高く、良く組織化されたパターンを抽出したものであることがわっかた。

WW(CW) では、中緯度の偏西風が弱まり（強まり）、その軸が北（南）へ移動し、その結果、日本近海上では東アジア冬季モンスーン（季節風）が弱まる（強まる）ことがわかった。このことは、西部北太平洋中緯度海域の冬季の海面水温は、強く東アジアモンスーンに支配されていることを確認するものである。また、赤道域では、28°C以上の高い海面水温の領域が、WWでは中央部から東部に位置しており、アノマリの場はENSO年のそれとよく似ていた。実際、WW(CW) として選択された冬季は、ENSO(ENSO+1) 年の冬季を含むが、ENSO+1(ENSO) 年冬季は含んでいない。

WWの風の応力場のアノマリに対する偏西風帯域での各冬季のアノマリの「相似度」の時系列は、気象庁が用いている極東東西指数の時系列と良い一致を示した。また、海面気圧場に対する同様な合成図解析から、WWとCWの偏西風の軸の南北変動は、アリューシャン低気圧の位置の顕著な南北変動に対応することがわっかた。